ORIGINAL PAPER

Improvement of electrochemical performance of $LiNi_{0.5}Co_{0.2}Mn_{0.3}O_2$ by LaF_3 coating at high cut-off voltage

Huapeng Yang[1] · Hailang Zhang[1] · Wentao Zhao[1]

Abstract

A simple wet chemical method was used to coat a layer of LaF_3 on the surface of $LiNi_{0.5}Co_{0.2}Mn_{0.3}O_2$(NCM523) to improve the electrochemical performance. Through the characterization of X-ray diffractometer (XRD), scanning electron microscope (SEM), X-ray energy dispersive spectrometer (EDS), and X-ray photoelectron spectroscopy (XPS), it can be seen that the LaF_3 coating can be uniformly coated on the surface of the material and will not change the crystal structure and micro-morphology of the material. In this work, the amount of LaF3 coating on the materials is 0.0 wt%, 0.5 wt%, 1.0 wt%, and 2.0 wt%, respectively. Under the condition of the optimum coating amount of 1 wt%, the rate performance and cycle performance of the coated material can be improved obviously. After 100 cycles at a high cut-off voltage of 4.6 V, the capacity retention of the 1 wt% LaF_3 coated material is 88.7%, which is higher than 80.4% of the bare material. And through EIS analysis, the coated material after 50 cycles still has excellent lithium ion diffusion kinetics. This may be due to the fact that an appropriate amount of LaF_3 coating can effectively avoid direct contact between cathode materials and electrolytes, inhibit the generation of oxygen vacancies, and reduce unnecessary side effects. This could provide a new idea for improving the electrochemical performance of $LiNi_{0.5}Co_{0.2}Mn_{0.3}O_2$ at high cut-off voltage.

Keywords Cathode material · $LiNi_{0.5}Co_{0.2}Mn_{0.3}O_2$ · LaF_3 coating · Electrochemical performance · High cut-off voltage

Introduction

Recently, with the continuous development of new energy field, lithium-ion battery (LIBs) has been widely used in portable electronic devices, electric vehicles (EVs), medical fields, and other fields because of its excellent energy density and safety performance [1–3]. However, the earlier commercial cathode materials, such as $LiMn_2O_4$ and $LiCoO_2$, have seriously limited the commercial application of lithium-ion batteries due to their poor high-voltage performance, unstable cycling performance, and low discharge specific capacity [4, 5].

Layered ternary cathode material $LiNi_xCo_yM_{1-x-y}O_2$ (NCM) has stable electrochemical performance and high energy density, making it an ideal cathode material for power

lithium-ion batteries [6, 7]. $LiNi_{0.5}Co_{0.2}Mn_{0.3}O_2$ (NCM523) has attracted more and more attention for its high initial discharge capacity, low cost, and high safety [8]. However, NCM523 has some defects in the commercial process, such as Li^+/Ni^{2+} mixing, long-period capacity attenuation, thermal instability, and gas escape [9]. The main reasons are as follows: (1) ion radii of Ni^{2+} and Li^+ are similar, which is easy to cause mixed discharge of cations. (2) Serious side reactions occur at the interface between the electrolyte and the positive electrode, which accumulates a large number of by-products on the surface of the positive electrode. (3) The surface of the cathode particles is unstable at high temperature, which leads to the rapid attenuation of the capacity during cycling. (4) The layered structure changes to electrochemically inert spinel or even salt facies at high cut-off voltage [10–14]. Therefore, some improvement measures need to be taken to improve the cyclic stability and rate performance. There are two common modification methods: the coating method and the doping method. Surface coating can effectively avoid direct contact between cathode materials and electrolytes to reduce side reactions. Typical coating materials include metal oxides TiO_2 [15], V_2O_5

✉ Hailang Zhang
zhl8868@vip.163.com

1 The Key Laboratory of Synthetic and Biological Colloids, Ministry of Education, School of Chemistry and Materials Engineering, Jiangnan University, Wuxi 214122, Jiangsu, People's Republic of China

[16], CeO_2 [17], fluorides CaF_2 [18] and AlF_3 [19], lithium ion conductor Li_2TiO_3 [20], Li_3VO_4 [21], phosphate $AlPO_4$ [22], and conductive polymer [23]. Zhao et al. obtained the precise Al_2O_3 coating on the surface of NCM523 by atomic layer deposition (ALD), which successfully inhibited the dissolution of TM during the NCM cycle and reduced the internal stress variation of NCM secondary particles during the cycle [24]. As a kind of rare earth fluoride, LaF_3 has good ionic conductivity, so it is often used as a modified material. In comparison, most oxides and phosphates react with electrolytes containing $LiPF_6$ to form corresponding fluoride, resulting in serious corrosion of cathode materials [25]. Therefore, fluoride as a coating material can effectively reduce the corrosion of HF to cathode materials in electrolyte, reduce the occurrence of side reactions, and effectively improve the cycle performance of materials, and fluoride is more stable than oxide in the ambient air, can effectively protect the cathode material, and reduce $LiOH/Li_2CO_3$ and other harmful impurities on the surface.

In this work, we used a simple wet coating method to coat the surface of $LiNi_{0.5}Co_{0.2}Mn_{0.3}O_2$ uniformly with LaF_3 and studied in detail the improvement of cycle performance and rate performance of LaF_3 coating on $LiNi_{0.5}Co_{0.2}Mn_{0.3}O_2$ cathode material at high cut-off voltage (4.6 V).

Experiments

Material synthesis

$LiNi_{0.5}Co_{0.2}Mn_{0.3}O_2$ cathode materials were synthesized by the coprecipitation method and high-temperature solid-state method. The chemicals used in this study are all analytical-grade reagents and can be used directly without further purification. The metal salts $NiSO_4 \cdot 6H_2O$, $CoSO_4 \cdot 7H_2O$, and $MnSO_4 \cdot H_2O$ were mixed into a solution (2.0 M) according to the molar ratio at 5:2:3, which was added into the reactor slowly and stirred continuously in a nitrogen atmosphere with the rotating speed of 300 rpm. At the same time, the NaOH (3.0 M) and ammonia (2.0 M) solutions, which are used as precipitators and complexing agents, were added into the reactor at a pH value of 11 (± 0.1) and kept the temperature at 55 °C. After the reaction, standing, washing, filtering, and drying at 120 °C for 24 h to obtain the precursor $Ni_{0.5}Co_{0.2}Mn_{0.3}(OH)_2$. The precursor and Li_2CO_3 were weighed and ground uniformly according to the molar ratio of 1:0.54, and then pre-sintered at 500 °C for 6 h, then calcined at 850 °C for 12 h, and finally the material $LiNi_{0.5}Co_{0.2}Mn_{0.3}O_2$ was obtained.

A certain amount of $LiNi_{0.5}Co_{0.2}Mn_{0.3}O_2$ was supersonic dispersed in ethanol and stirred by magnetic force at 30 °C for 1 h. The configured NH_4F and $La(NO_3)_3 \cdot H_2O$ solution were added slowly into the reactor, and the mole ratio was strictly

controlled at 3:1. Subsequently, the mixed solution was heated to 65 °C and stirred quickly until all the solution was volatilized. The prepared samples were dried in a vacuum at 120 °C for 12 h and then calcined in air at 400 °C for 5 h. In order to explore the optimal coating amount, the prepared LaF_3 coating amount is 0.0 wt%, 0.5 wt%, 1.0 wt%, and 2.0 wt%, respectively, marked as LF0, LF0.5, LF1, and LF2.

Material characterization

The structure of the sample was analyzed by X-ray diffractometer (XRD, Advance D8). The sample was collected in the 2θ range of 10~90°, and the scanning rate was 5°/min. In order to analyze the surface morphology and element distribution of the sample, the morphology and microstructure of the material were observed by S4800 scanning electron microscope (SEM), and the coating of elements on the original sample surface was detected by X-ray energy dispersive spectrometer (EDS, Noran System Six, USA). The thickness of the coating was observed by JEOL JEM2100F transmission electron microscope (TEM). The oxidation state of elements in the material was examined by X-ray photoelectron spectroscopy (XPS, Thermo K-alpha).

Electrochemical test

The positive active material, acetylene black (Super P), and polyvinylidene fluoride (PVDF) were uniformly mixed and ground according to the mass ratio of 8:1:1, and the proper amount of organic solvent N-methyl pyrrolidone (NMP) was added. The obtained slurry was uniformly coated on the aluminum foil with a Doctor blade technique and dried in a vacuum at 80 °C for 12 h. The electrode with a diameter of 14 mm was prepared by pressing and punching. The button battery (CR2032) was assembled in a glove box filled with argon with an electrode piece as the positive electrode, a metal lithium piece as the negative electrode, Celgard2325 PP microporous diaphragm and 1 mol·L^{-1} $LiPF_6$ [EC + DMC + EMC (v: v: v = 1:1:1)] solution as the electrolyte. The constant current charge–discharge cycle test was carried out by using the LAND battery test system (CT2001A, Wuhan in China) at 25 °C. Cyclic voltammetry test (voltage range 2.5~4.6 V, scanning rate 150 μV/S) and impedance test were carried out on electrochemical workstation (IM6E, Zahenr, Germany), with a frequency range of 100 kHz~0.01 Hz and amplitude of 5 mV.

Results and discussion

Microstructural characterization

Figure 1a shows the XRD patterns of bare NCM523 and NCM523 with different LaF_3 coating amounts. It can be seen

Fig. 1 **A**, **b** XRD diffraction patterns of cathode materials and the magnification of the (003) peak. **c**, **d** XRD refinement of LF0 and LF1
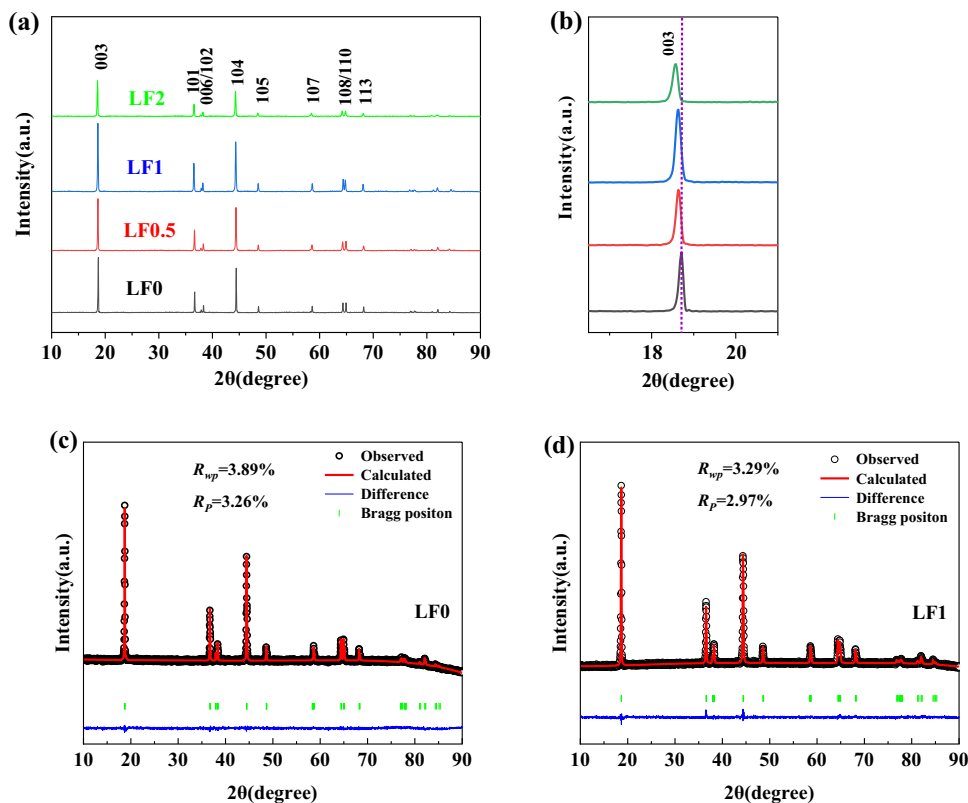

Table 1 Rietveld refinement lattice parameters of original and LaF$_3$ coated NCM523 samples

Samples	a/Å	c/Å	c/a	I_{003}/I_{104}	Li/Ni disorder
LF0	2.86991	14.23199	4.959	1.24	0.0524
LF0.5	2.87078	14.24885	4.963	1.32	0.0485
LF1	2.87291	14.25478	4.962	1.36	0.0408
LF2	2.87453	14.25532	4.959	1.35	0.0466

that all the materials have two clear splitting peaks of (006)/(102) and (108)/(110), indicating that the layered structure of the four materials is sequential and showing a single hexagonal α-NaFeO$_2$ structure and R-3 m space group [26, 27]. It can be seen from Fig. 1b that the (003) peak shifts obviously to the left after coating, which indicates that the lattice parameters increase. Tables 1, 2 lists the unit cell parameters

after Rietveld refinement, and the c/a values of all samples are greater than 4.9, indicating that the layered structure of the materials is good. In addition, the ratio of $I_{(003)}/I_{(104)}$ of LF1 is 1.36, which is higher than that of the bare sample (1.24), indicating that the LaF$_3$ coating may reduce the mixing of cations and could improve the structural stability of the active materials [28]. There are no other impurity peaks in the XRD spectra of the coated samples, which indicate that the LaF$_3$ coating will not change the crystal structure of the material.

In order to further study the effect of LaF$_3$ coating on the morphology of NCM523, the SEM diagrams of LF0, LF0.5, LF1, and LF2 were compared. As shown in Fig. 2, it can be clearly observed that the samples are composed of submicron particles with an average particle size of about 12 μm, which is approximately spherical, and there is no obvious agglomeration. The surface of the sample LF0 is

Table 2 Electrochemical data of the pristine and LaF$_3$-coated LiNi$_{0.5}$Co$_{0.2}$Mn$_{0.3}$O$_2$ samples

Sample	Initial charge capacity at 0.1 C (mAh·g^{-1})	Initial discharge capacity at 0.1 C (mAh·g^{-1})	Coulombic efficiency (%)	100th discharge capacity at 0.5 C (mAh·g^{-1})	Capacity retention (%)
LF0	231.9	190.7	82.2	147.6	80.3
LF0.5	227.8	188.9	82.9	154.2	83.2
LF1	216.9	187.1	86.3	163.6	88.7
LF2	235.7	185.1	78.5	152.5	84.4

smooth, and there are no particles attached. However, the surface of the sample coated with LaF$_3$ becomes rough, there are particles attached, and most of the angular features become blurred. And with the increase of the amount of coating, it is difficult to distinguish the gaps between the primary particles. Too many coating materials will hinder the deintercalation/intercalation of lithium ions, resulting in a decrease in capacity. Figure 3 shows the EDS pattern of the LF1 sample to test the uniformity of the elements on the sample surface. As shown in Fig. 3a–g, Mn, Ni, Co, O, La, and F elements are uniformly distributed on the surface of the particles, indicating that LaF$_3$ is uniformly coated on the surface of NCM523, which will play an effective role in the cyclic stability.

Figure 4 shows the TEM image of LF1. It can be seen that the surface of NCM523 is coated with a layer of LaF$_3$ with a thickness of about 5 nm. The uniform coating can effectively prevent the electrode material from direct contacting with the electrolyte and reduce unnecessary side reactions. Figure 4a is an enlarged view of the yellow area in Fig. 4b, and an obvious lattice stripe, about 0.461 nm, can be observed, corresponding to the (003) crystal plane of LiNO$_2$, which indicates that the LaF$_3$ coating will not change the microstructure of the sample and still maintains the layered structure [29].

In order to analyze the chemical valence of each element in the sample, LF1 was tested by XPS. In Fig. 5a, the whole spectrum shows obvious peaks of Mn, Co, Ni, F, and La, and no other impurities exist. Figure 5b–f shows the measured spectra of each element. The Mn-XPS spectrum

has two main peaks including Mn 2p$_{3/2}$(641.4 eV) and Mn 2p$_{1/2}$(653.1 eV), which indicates that the chemical state of Mn in the sample is Mn^{4+} [30]. The peaks around 855.9 eV and 873.3 eV belong to Ni 2p$_{3/2}$ and Ni 2p$_{1/2}$ [31]. The peaks of 779.8 eV and 794.08 eV belong to Co 2p$_{3/2}$ and Co 2p$_{1/2}$, indicating that the main valence state of Co is + 3 [32]. Figure 5e shows that there is a main peak at 684.08 eV, which corresponds to F 1 s. Such value revealed that the F valence was − 1 [33]. In Fig. 5f, the peak at 834.34 eV corresponds to 3d$_{5/2}$ of La^{3+} [34]. This indicates that the NCM523 sample was effectively coated by LaF$_3$.

Electrochemical performance

In order to test the effect of LaF$_3$ coating on the electrochemical performance of cathode materials, LF0, LF0.5, LF1, and LF2 were assembled into button cells for charge and discharge tests. Figure 6a shows the initial charge–discharge curve of cathode materials with different LaF$_3$ coating amount at 0.1 C (1 C = 180 mAh·g^{-1}), 3.0–4.6 V. The curves of all samples are similar and smooth, and the discharge platform is about 3.8 V. With the increase of coating amount, the discharge specific capacity of cathode materials decreases in varying degrees. The bare material has the highest discharge specific capacity of 190.7 mAh·g^{-1}, while the discharge specific capacity of LF0.5, LF1, and LF2 is 188.9, 187.1, and 185.1 mAh·g^{-1}, respectively, which are lower than that of LF0. This is because LaF$_3$ is an inert material; no additional discharge specific capacity can be provided. However, LF1 has the highest

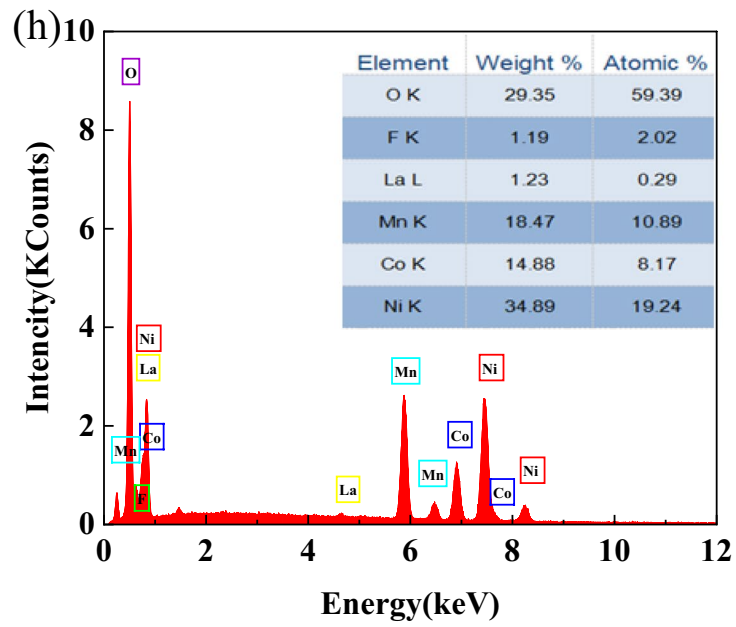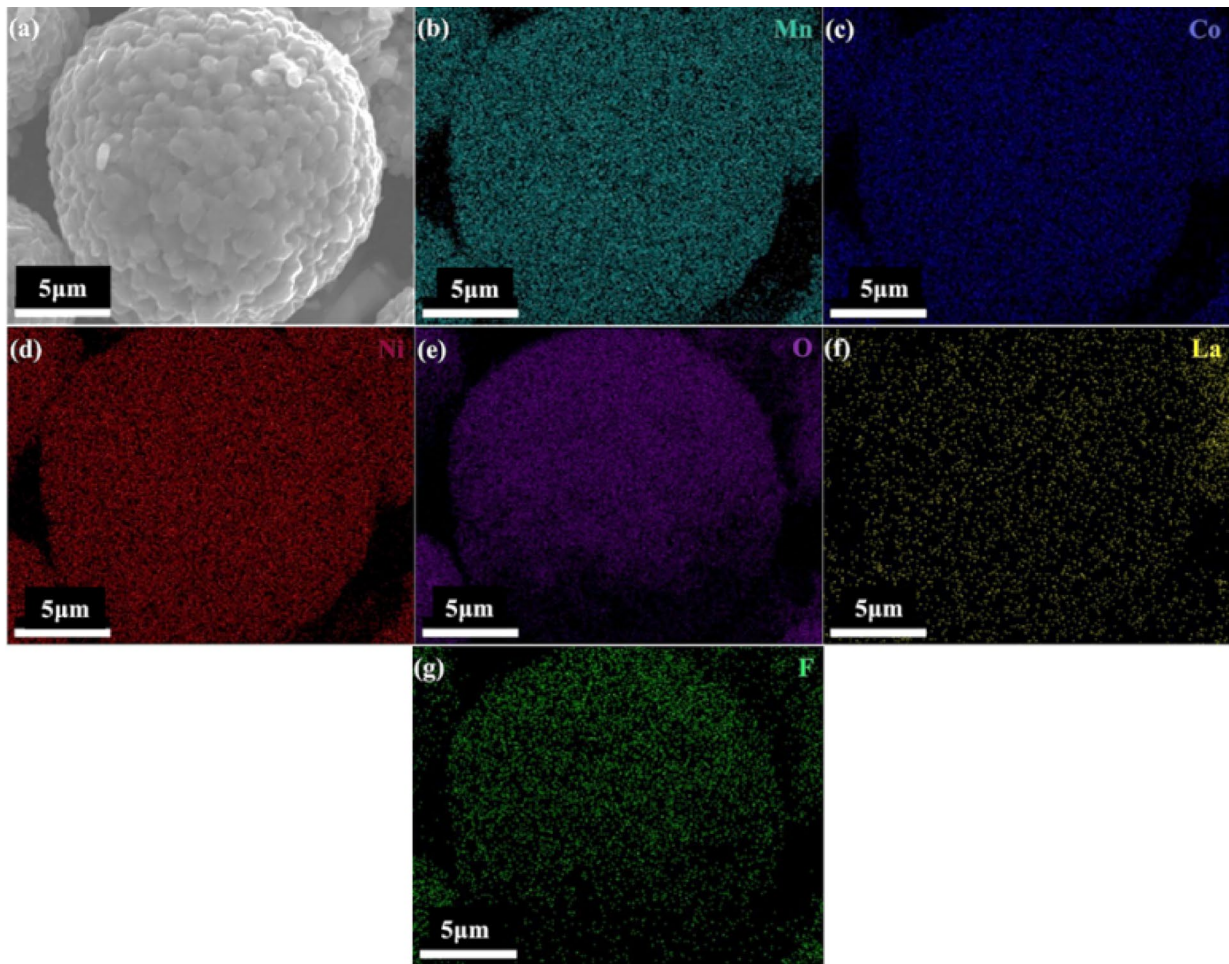**Fig. 2** SEM diagrams of cathode materials with different LaF$_3$ coating amount
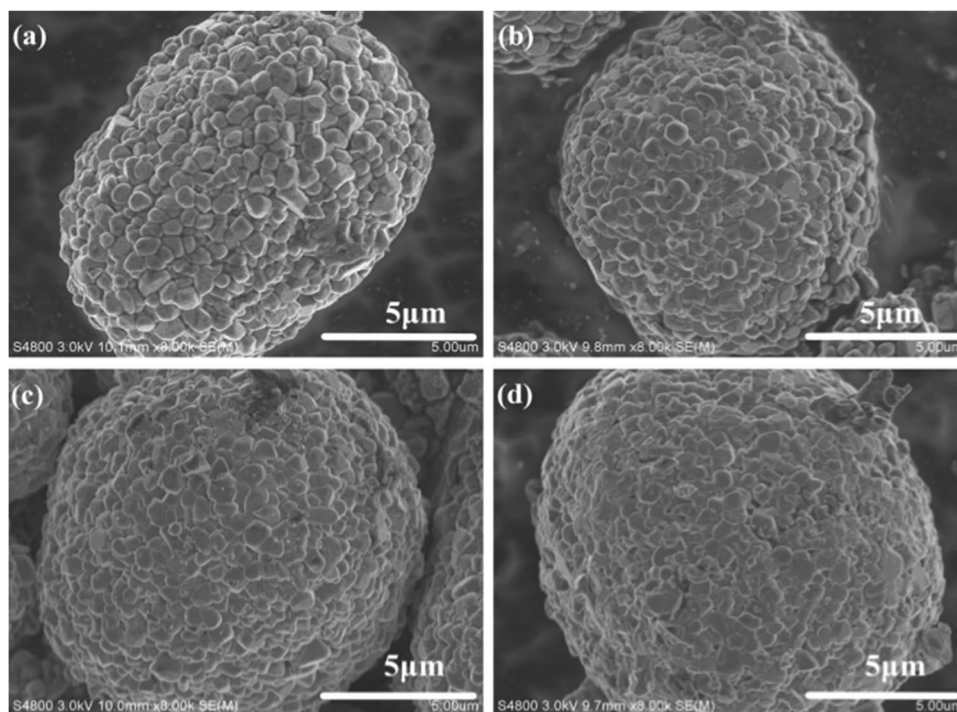
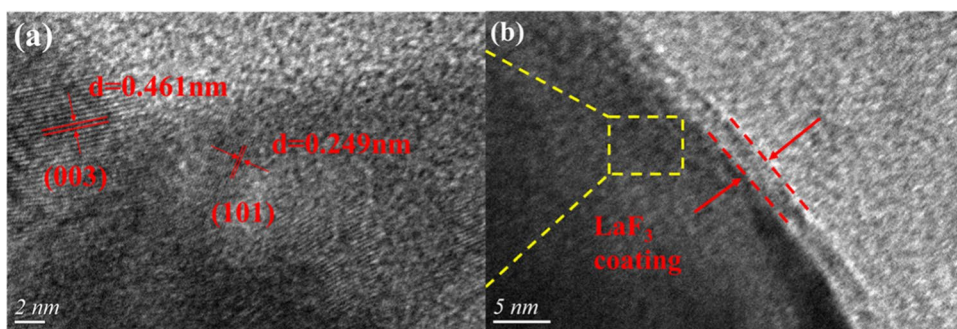**Fig. 3** EDS mapping of LF1 particle surface

Fig. 4 TEM image of LF1

Fig. 5 X-ray photoelectron spectroscopy for LF1, **a** survey spectrum, **b** Mn 2p, **c** Co 2p, **d** Ni 2p, **e** F 1 s, and **f** La 3d
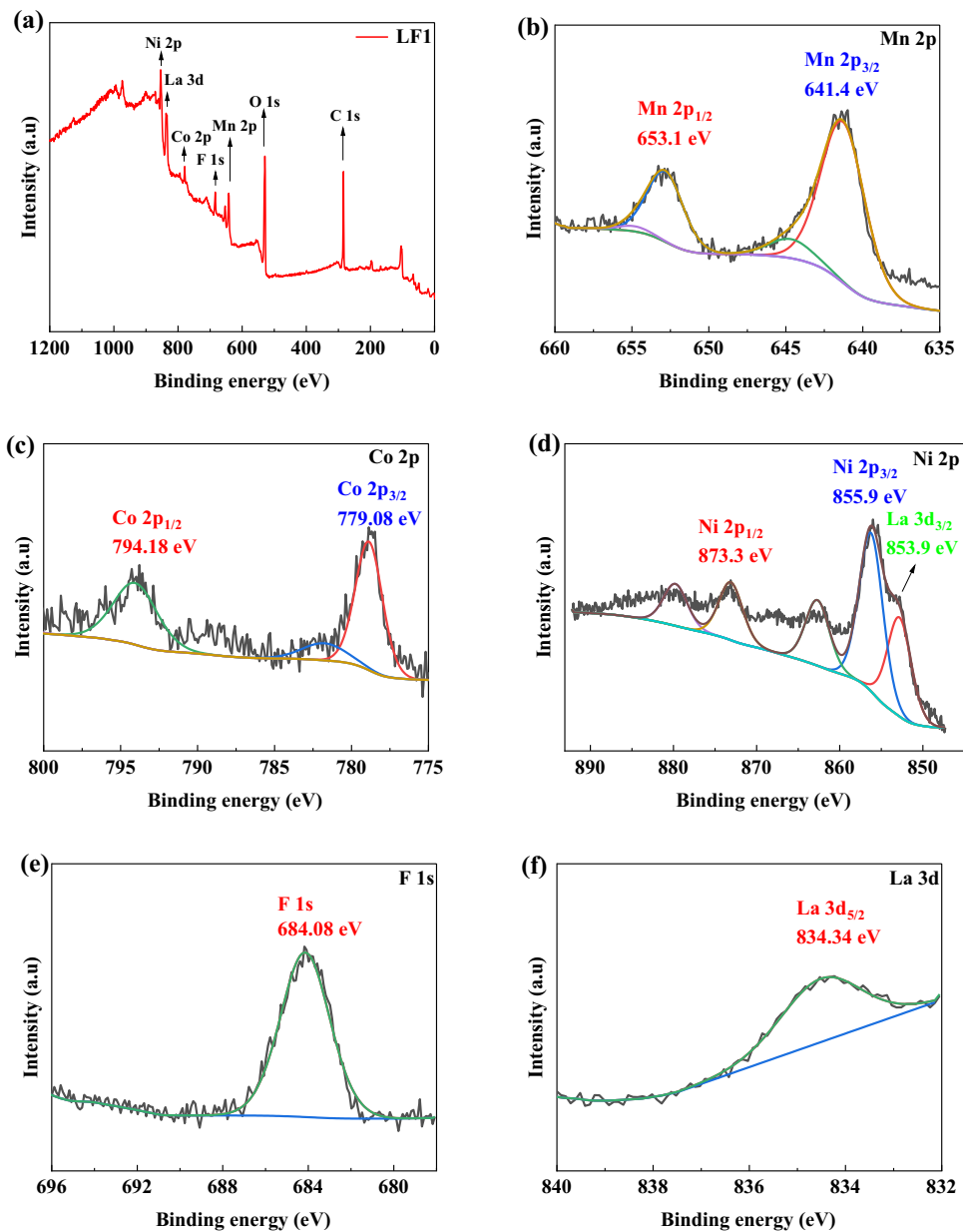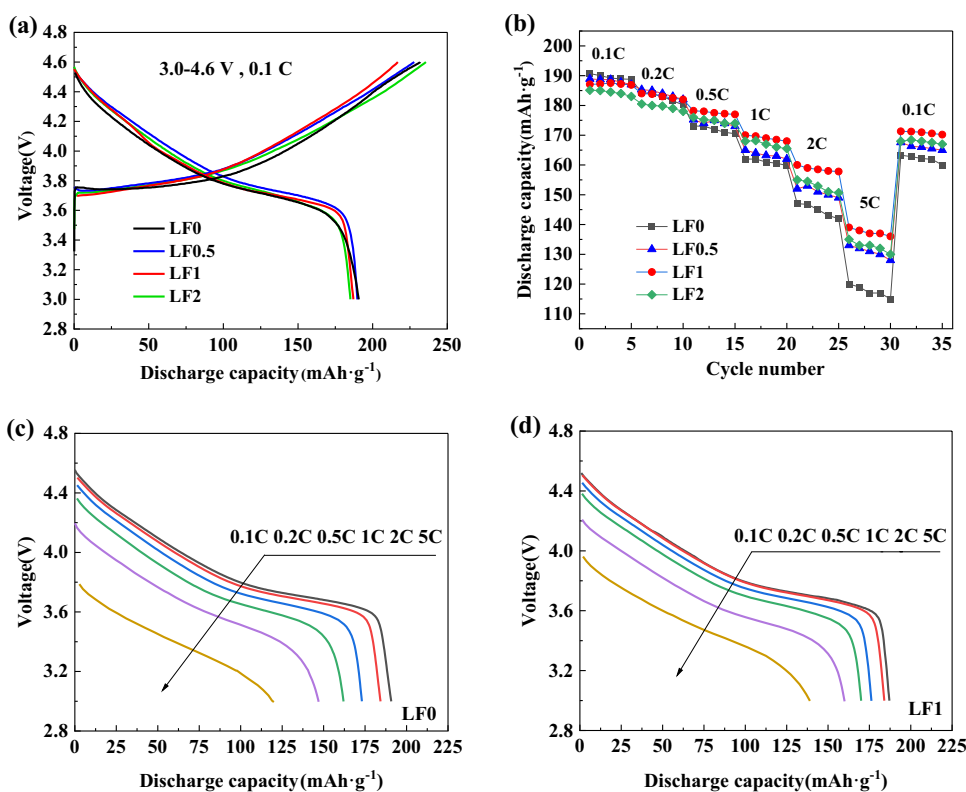
Fig. 6 A Initial charge–discharge curves of LF0, LF0.5, LF1, and LF2 at 3.0–4.6 V 0.1 C. **b** Rate performance of NCM523 with different LaF$_3$ coating. **c, d** Discharge curves of LF0 and LF1 at different rates

coulombic efficiency (86.3%), which is significantly higher than that of bare samples (82.2%). This is due to the fact that an appropriate amount of coating can prevent direct contact between electrodes and electrolytes, thus improving coulombic efficiency [35]. However, the thicker coating of LF2 reduces the mass of active material and hinders the diffusion of lithium ion, which leads to the decrease of discharge specific capacity.

Figure 6b–d depicts the rate performance of LF0, LF0.5, LF1, LF2, and the discharge curves of LF0 and LF1 at different rates. All materials were cycled 5 times at 0.1, 0.2, 0.5, 1, 2, and 5 C, respectively, and then recovered to 0.1 C at 3.0–4.6 V. At low current density (0.1 C and 0.2 C), the original sample still has higher discharge specific capacity and smaller attenuation, which is slightly higher than that of the coated material. However, with the increase of current density, the capacity of the bare sample began to decrease rapidly, especially at 5 C; the capacity of the original sample was only 120.0 mAh·g^{-1}, while the discharge capacities of LF0.5, LF1, and LF2 at 5 C were 133.1, 139.4, and 135.2 mAh·g^{-1}, respectively, mainly due to the increase of polarization. In addition, when the current is restored to 0.1 C, LF1 can still maintain a discharge specific capacity of 91.5% (171.3 mAh·g^{-1}), which shows that LF1 has good reversibility. The discharge capacity retention rates of LF0, LF0.5, and LF2 at 0.1 C were 85.6% (163.3 mAh·g^{-1}), 88.7% (167.6 mAh·g^{-1}), and 90.8% (168 mAh·g^{-1}), respectively. The

results show that an appropriate amount of LaF$_3$ coating can improve the high-rate cycle performance.

In order to further explore the improvement of the electrochemical performance of NCM523 coated by LaF$_3$, the cycle performance of LF0, LF0.5, LF1, and LF2 was tested at 25 °C. The cycle performance was tested at 0.5 C. As shown in Fig. 7a, after 100 cycles, the discharge specific capacities of LF0, LF0.5, LF1, and LF2 are 147.6, 154.2, 163.6, and 152.5 mAh·g^{-1}, respectively, and the retention rates are 80.4%, 83.2%, 88.7%, and 84.4%, respectively. By comparison, it is obvious that the cycle performance of LF0 is the worst, which is mainly due to the corrosion of HF to the cathode material and the accumulation of a large number of by-products on the surface of the material. The main reactions are as follows:

$$LiPF_6 \rightarrow LiF + PF_5 \tag{1}$$

$$PF_5 + H_2O \rightarrow POF_3 + 2HF \tag{2}$$

And at a high cut-off voltage of 4.6 V, the reaction will be accelerated, which leads to the rapid attenuation of the discharge capacity. However, the cycle stability of LF1 is the best, which shows that an appropriate amount of LaF$_3$ surface modification layer can effectively restrain the generation of oxygen vacancy and alleviate the corrosion of electrolyte to the material. In order to observe the redox reaction in

Fig. 7 **A** Cycle performance of NCM523 with different LaF$_3$ coating at 3.0–4.6 V 0.5 C. **b**, **c** dQ/dV curves of cycles 1, 25, and 50 of LF0 and LF1 at 3.0–4.6 V. **d** Cyclic voltammograms of LF0 and LF1
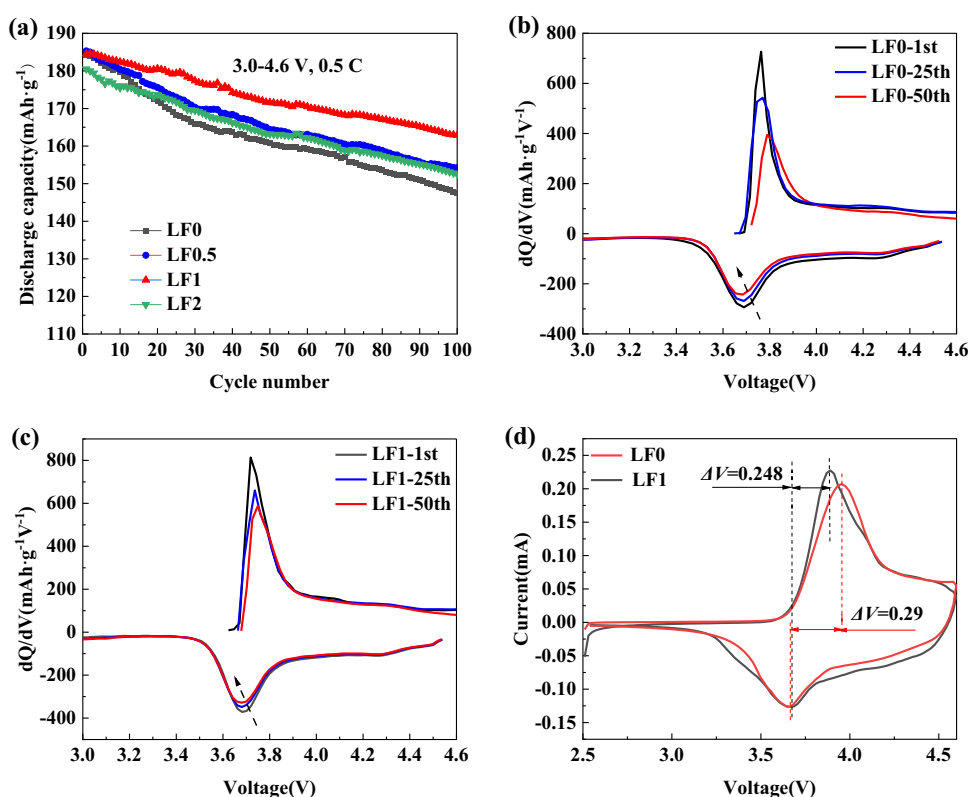
detail during the cycle, the differential capacity curve (dQ/dV) curves of LF0 and LF1 at lap 1, 25, and 50 were drawn respectively. As shown in Fig. 7b, c, all materials show typical anodic peaks around 3.7–3.8 V. With the increase of the number of cycles, the oxidation peak of the sample shifts to the right and the reduction peak shifts to the left. It can be observed that the potential difference of LF1 is obviously smaller than that of LF0. This shows that the coated sample can better maintain the redox peak and eliminate the kinetic

energy barrier of electrochemical redox reaction, thus reducing the capacity attenuation [36].

Cyclic voltammograms and electrochemical impedance spectroscopy

In order to determine the charge–discharge reaction process and analyze the mechanism of its improvement, LF0 and LF1 were tested by cyclic voltammetry. Figure 7d is the CV

Fig. 8 **A** Nyquist curve of LF0 and LF1 samples at 3.0–4.6 V, 0.5 C after cycles 3 and 50. **b** The relationships between Z' and $\omega^{-0.5}$ based on the 3rd cycle c and 50th cycle. **c** The equivalent circuit model
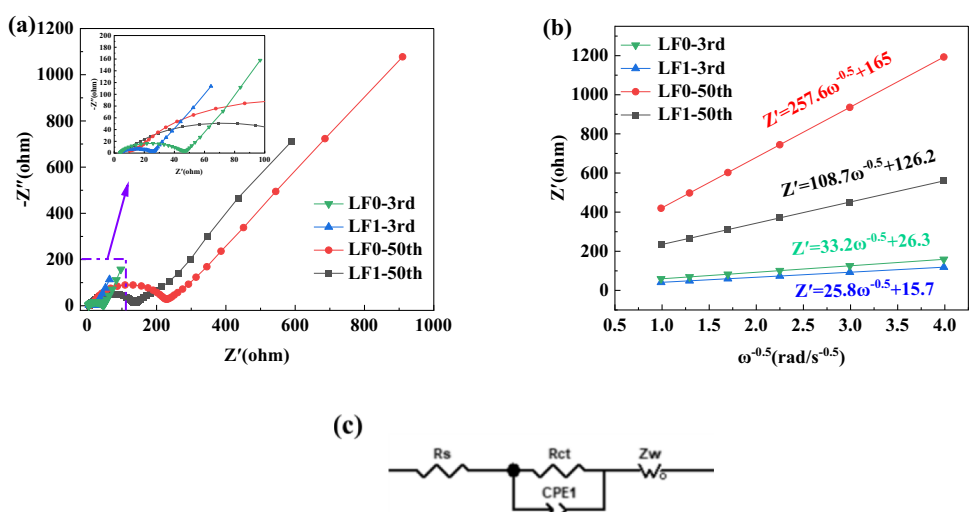
Table 3 Impedance and lithium ion diffusion coefficient of LF0 and LF1 samples after the 3rd and 50th cycles

Specimen	3rd			50th		
	R_s/Ω	R_{ct}/Ω	$D_{Li}/cm^2 \cdot s^{-1}$	R_s/Ω	R_{ct}/Ω	$D_{Li}/cm^2 \cdot s^{-1}$
LF0	3.738	38.98	1.08×10^{-12}	11.71	223.3	1.79×10^{-14}
LF1	2.998	19.75	1.79×10^{-12}	4.089	118.6	1.01×10^{-13}

diagrams. It can be seen that the oxidation peaks of LF0 and LF1 are 3.954 V and 3.891 V, respectively, and the corresponding reduction peaks are 3.664 V and 3.643 V, respectively. The potential difference can reflect the polarization and cyclic reversibility of the electrode. The potential difference of LF0 is 0.29 V, which is significantly larger than the 0.248 V of LF1. This shows that LaF_3-modified NCM523 has a lower degree of polarization, which is corresponding to its excellent rate performance and cyclic performance [22].

Electrochemical impedance spectroscopy (EIS) was performed to further analyze the electrochemical kinetic characteristics of LF0 and LF1 after 3 cycles and 50 cycles at 3.0–4.6 V, 0.5 C. As shown in Fig. 8a, each curve of the impedance spectrum consists of a semicircle and a straight line, and the frequency range is from 0.01 Hz to 100 kHz. The first intersection of the curve with the Z' represents the solution impedance (R_s), which includes solution resistance and diaphragm resistance. The semicircle in the intermediate frequency region represents the charge transfer resistance (R_{ct}), which refers to the resistance encountered when Li^+ passes through the double layer, and is related to the dynamic characteristics of lithium batteries. The diagonal part is related to

the Warburg resistance and the diffusion impedance of lithium ion in the electrode. The impedance is fitted by Z-view software, and the calculated fitting value is shown in Table 3. It can be seen that the charge transfer resistance R_{ct} of LF0 after 3 cycles is 38.98 Ω, which is larger than 19.75 Ω of LF1, and after 50 cycles, the R_{ct} of LF0 increases rapidly to 223.3 Ω, while the R_{ct} of LF1 is only 118.6 Ω, which is much smaller than that of bare samples. This is due to the dissolution of transition metal ions in the bare materials during the cycle, the transition of layered structure to spinel salt phase, and the increase of surface impedance, thus hindering the diffusion of Li^+ [13, 37]. This shows that LaF_3 coating can well protect the electrode material, reduce the occurrence of side reactions, and prevent the attack of HF. There is a slight change in R_s during the cycle, which indicates that the solution resistance is little affected [18].

The diffusion coefficient of lithium ion can also be calculated by impedance diagram, and the formula is as follows:

$$D_{Li^+} = \frac{R^2 T^2}{2n^4 F^4 C_{Li}^2 A_c^2 \sigma^2} \tag{3}$$

Fig. 9 SEM images of LF0 (**a**, **b**) and LF1 (**c**, **d**) after 100 cycles at 3.0–4.6 V
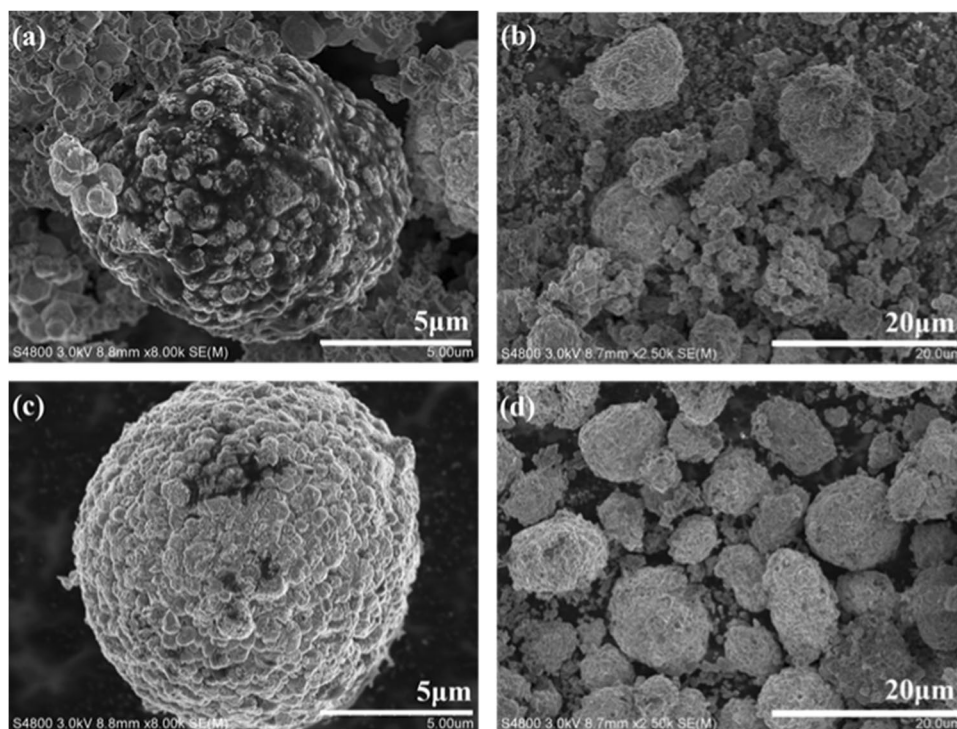
$$Z' = R_s + R_{ct} + \not\exists\tilde{}\not\exists^{\circ-0.5} \tag{4}$$

In the above formula, R is the gas constant, T is the absolute temperature, n is the number of transferred electrons, F is the Faraday constant, C_{Li} is the molar concentration of lithium ion, Ac is the positive electrode area, and σ is the Warburg coefficient fitted by $\omega^{-0.5}$ and Z'. Figure 8b shows the equations fitted by $\omega^{-0.5}$ and Z' in circles 3 and 50, respectively. The lithium ion diffusion coefficients of LF0 in the third and 50th circles are calculated to be 1.08×10^{-12} and 1.79×10^{-14} cm$^2\cdot$s^{-1}, respectively, while the lithium ion diffusion coefficients of LF1 in the third and 50th circles are 1.79×10–12 and 1.01×10–13 cm$^2\cdot$s^{-1}, respectively, which are higher than those of the bare samples. This is due to the corrosion of the bare sample by HF, which shows that a large number of by-products are accumulated in the material, which seriously affects the diffusion of lithium ion, while an appropriate amount of LaF$_3$ coating can effectively protect the cathode material from crystal collapse and still has excellent lithium ion diffusion kinetics.

Figure 9a–d show the SEM images of the LF0 and LF1 after 100 cycles at 3.0–4.6 V. Part of the spherical shape of the pristine particles was destroyed, and micro-cracks appeared on the surface, accompanied by a large number of scattered fragments. This is mainly due to the direct contact between the pristine particles and the electrolyte, which leads to the lattice corrosion, while LF1 is still mostly compact spherical secondary particles, with few scattered fragments. LaF$_3$ coating can not only be used as a protective layer, but also shield HF in electrolyte. The results show that the structure and interface stability of NCM523 are greatly improved after LaF$_3$ coating, which corresponds to its excellent cycle performance [24, 38].

Conclusion

The cathode material LiNi$_{0.5}$Co$_{0.2}$Mn$_{0.3}$O$_2$ was prepared by coprecipitation and high-temperature solid-state method, and a layer of LaF$_3$ material was uniformly coated on the surface of the material by the wet chemical method. In this work, the amount of LaF3 coating on the materials is 0.0 wt%, 0.5 wt%, 1.0 wt%, and 2.0 wt%, respectively. Uniform LaF$_3$ coating can effectively inhibit the formation of residual alkali on the cathode material and isolate the cathode material from the electrolyte to resist HF attack. At high rate, the capacity decay of uncoated samples is significantly faster than that of coated samples, and when returning to low rate, 1 wt% coated samples still have a capacity retention of 91.5%, while uncoated samples have only 85.6%. Through CV and EIS diagrams, it can be found that LaF$_3$ coating can significantly reduce the electrochemical polarization and charge transfer resistance, which corresponds to

its excellent rate performance and cycle performance. However, LaF$_3$ coating can not provide an additional discharge capacitance, resulting in an initial discharge capacity slightly lower than that of the bare sample, which still needs further improvement.

References

1. Li M, Lu J, Chen Z, Amine K (2018) 30 years of lithium-ion batteries. Adv Mater 1800561:1–24
2. Zhou H, Xin F, Pei B, Whittingham MS (2019) What limits the capacity of layered oxide cathodes in lithium batteries? ACS Energy Lett 4:1902–1906
3. Zha Q, Hu N, Song C, Hou H, Liao S, Zha G (2021) Improving cycle stability of Ni-rich LiNi$_{0.8}$Mn$_{0.1}$Co$_{0.1}$O$_2$ cathode materials by Li$_4$Ti$_5$O$_{12}$ coating. Ionics 28:1047–1054
4. Krishna KS, Ghosh S, Ghosal P, Martha SK (2017) Synergistic effect of 3D electrode architecture and fluorine doping of Li$_{1.2}$Ni$_{0.15}$Mn$_{0.55}$Co$_{0.1}$O$_2$ for high energy density lithium-ion batteries. J Power Sources 356:115–123
5. Song L, Li X, Xiao Z, Li L, Cao Z, Zhu H (2018) Effect of Zr doping and Li$_2$O-2B$_2$O$_3$ layer on the structural electrochemical properties of LiNi$_{0.5}$Co$_{0.2}$Mn$_{0.3}$O$_2$ cathode material: experiments and first-principle calculations. Ionics 25:2017–2026
6. Zhang Z, Qiu J, Yu M, Jin C, Yang B, Guo G (2020) Performance of Al-doped LiNi$_{1/3}$Co$_{1/3}$Mn$_{1/3}$O$_2$ synthesized from spent lithium ion batteries by sol-gel method. Vacuum 172
7. Choi NS, Han J-G, Ha SY, Park I, Back CK (2015) Recent advances in the electrolytes for interfacial stability of high-voltage cathodes in lithium-ion batteries. RSC Adv 5:2732–2748
8. Bak SM, Hu E, Zhou Y, Yu X, Senanayake SD, Cho SJ, Kim KB, Chung KY, Yang XQ, Nam KW (2014) Structural changes and thermal stability of charged LiNi$_x$Mn$_y$Co$_z$O$_2$ cathode materials studied by combined in situ time-resolved XRD and mass spectroscopy. ACS Appl Mater Interfaces 6:22594–22601
9. Liu BS, Zhang SH, Yu YG, Liu JH, He X, Sun ZJ, Yu ZQ, Wu YM, Wang ZB (2021) Interface crystal domain regulation via TiO$_2$ surface modification enhancing stability of layered LiNi$_{0.5}$Co$_{0.2}$Mn$_{0.3}$O$_2$ for lithium-ion batteries. Ionics 27:1871–1880
10. Zhang H, Zhang Y, Xu T, John AE, Li Y, Li W, Zhu B (2016) Poly(m-phenylene isophthalamide) separator for improving the heat resistance and power density of lithium-ion batteries. J Power Sources 329:8–6
11. He M, Su CC, Peebles C, Feng Z, Connell JG, Liao C, Wang Y, Shkrob IA, Zhang Z (2016) Mechanistic insight in the function of phosphite additives for protection of LiNi$_{0.5}$Co$_{0.2}$Mn$_{0.3}$O$_2$ cathode in high voltage Li-ion cells. ACS Appl Mater Interfaces 8:11450–11458
12. Liu T, Zhao SX, Wang KZ, Gou LL, Nan CW (2015) Improved rate capability and cycle stability of Li[Ni$_{0.5}$Co$_{0.2}$Mn$_{0.3}$]O$_2$ with Li$_2$MnO$_3$ coating under high cut-off voltage. Appl Surf Sci 355:1222–1228
13. Liu W, Oh P, Liu X, Lee MJ, Cho W, Chae S, Kim Y, Cho J (2015) Nickel-rich layered lithium transition-metal oxide for high-energy lithium-ion batteries. Angew Chem Int Ed Engl 54:4440–4457
14. Li GY, Zhang ZJ, Wang R, Hung ZL, Zuo ZC, Zhou HH (2016) Effect of trace Al surface doping on the structure, surface chemistry and low temperature performance of LiNi$_{0.5}$Co$_{0.2}$Mn$_{0.3}$O$_2$ cathode. Electrochim Acta 212:399–407

15. Li Y, Liu X, Ren D, Hsu H, Xu GL, Hou J, Wang L, Feng X, Lu L, Xu W, Ren Y, Li R, He X, Amine K, Ouyang M (2020) Toward a high-voltage fast-charging pouch cell with TiO_2 cathode coating and enhanced battery safety. Nano Energy 71:104643

16. Yuan M, Li Y, Chen Q, Chen C, Liu X, Zeng W, Wang R, Xiao S (2019) Surfactant-assisted hydrothermal synthesis of V_2O_5 coated $LiNi_{1/3}Co_{1/3}Mn_{1/3}O_2$ with ideal electrochemical performance. Electrochim Acta 323:134822

17. Zhou LJ, Yin ZL, Ding ZY, Li XH, Wang ZX, Guo HJ (2017) CeO_2 coating to improve the performance of $Li[Li_{0.2}Mn_{0.54}Ni_{0.13}Co_{0.13}]O_2$. Ionics 24:2533–2542

18. Dai S, Yan G, Wang L, Luo L, Li Y, Yang Y, Liu H, Liu Y, Yuan M (2019) Enhanced electrochemical performance and thermal properties of Ni-rich $LiNi_{0.8}Co_{0.1}Mn_{0.1}O_2$ cathode material via CaF_2 coating. J Electroanal Chem 847:113197

19. Kim HB, Park BC, Myung ST, Amine K, Prakash J, Sun YK (2008) Electrochemical and thermal characterization of AlF_3-coated $Li[Ni_{0.8}Co_{0.15}Al_{0.05}]O_2$ cathode in lithium-ion cells. J Power Sources 179:347–350

20. Xiong F, Chen Z, Huang C, Wang T, Zhang W, Yang Z, Chen F (2019) Near-equilibrium control of Li_2TiO_3 nanoscale layer coated on $LiNi_{0.8}Co_{0.1}Mn_{0.1}O_2$ cathode materials for enhanced electrochemical performance. Inorg Chem 58:15498–15506

21. Huang Y, Jin FM, Chen FJ, Chen L (2014) Improved cycle stability and high-rate capability of Li_3VO_4-coated $Li[Ni_{0.5}Co_{0.2}Mn_{0.3}]O_2$ cathode material under different voltages. J Power Sources 256:1–7

22. Wang JH, Wang Y, Guo YZ, Liu CW, Dan LL (2014) Electrochemical characterization of $AlPO_4$ coated $LiNi_{1/3}Co_{1/3}Mn_{1/3}O_2$ cathode materials for high temperature lithium battery application. Rare Met 40:78–83

23. Liu X, Li H, Li D, Ishida M, Zhou H (2013) PEDOT modified $LiNi_{1/3}Co_{1/3}Mn_{1/3}O_2$ with enhanced electrochemical performance for lithium ion batteries. J Power Sources 243:374–380

24. Cao G, Jin Z, Zhu J, Li Y, Xu B, Xiong Y, Yang J (2020) A green Al_2O_3 metal oxide coating method for $LiNi_{0.5}Co_{0.2}Mn_{0.3}O_2$ cathode material to improve the high voltage performance. J Alloys Compd 832:153788

25. Xiong X, Wang Z, Guo H, Zhang Q, Li X (2013) Enhanced electrochemical properties of lithium-reactive V_2O_5 coated on the $LiNi_{0.8}Co_{0.1}Mn_{0.1}O_2$ cathode material for lithium ion batteries at 60 ℃. J Mater Chem A 1:1284–1288

26. Wang D, Li XH, Wang ZX, Guo HJ, Xu Y, Fan YL, Ru JJ (2016) Role of zirconium dopant on the structure and high voltage electrochemical performances of $LiNi_{0.5}Co_{0.2}Mn_{0.3}O_2$ cathode materials for lithium ion batteries. Electrochim Acta 188:48–56

27. Li Z, Cao S, Xie X, Wu C, Li H, Chang B, Chen G, Guo X, Zhang X, Wang X (2021) Boosting electrochemical performance of lithium-rich manganese-based cathode materials through a dual modification strategy with defect designing and interface engineering. ACS Appl Mater Interfaces 13:53974–53985

28. Chen Z, Chao D, Chen M, Shen Z (2020) Hierarchical porous $LiNi_{1/3}Co_{1/3}Mn_{1/3}O_2$ with yolk-shell-like architecture as stable cathode material for lithium-ion batteries. RSC Adv 10:18776–18783

29. Habibi A, Jalaly M, Rahmanifard R, Ghorbanzadeh M (2020) Microwave-reduced graphene oxide wrapped NCM layered oxide as a cathode material for Li-ion batteries. J Alloy Compd 834:155014

30. Chen XL, Lu WZ, Chen C, Xue MZ (2018) Improved electrochemical performance of $LiNi_{0.5}Co_{0.2}Mn_{0.3}O_2$ cathode with different carbon additives for lithium-ion batteries. Int J Electrochem Sci 13:296–304

31. Huang B, Wang M, Yang X, Xu G, Gu Y (2019) Enhanced electrochemical performance of the layered nickel-rich oxide cathode by $KMnO_4$ treatment precursor. J Alloy Compd 808:151683

32. Feng L, Liu Y, Qin W, Yang Z, Liu J (2021) A novel double modification to enhance electrochemical performance of $LiNi_{0.5}Co_{0.2}Mn_{0.3}O_2$ by substituting Ce for Co site. Electrochim Acta 391:138904

33. Zhang M, Wang C, Zhang J, Li G, Gu L (2021) Preparation and electrochemical characterization of La and Al Co-doped NCM811 cathode materials. ACS Omega 6:16465–16471

34. Li YC, Zhao WM, Xiang W, Wu ZG, Yang ZG, Xu CL, Xu YD, Wang EH, Wu CJ, Guo XD (2018) Promoting the electrochemical performance of $LiNi_{0.8}Co_{0.1}Mn_{0.1}O_2$ cathode via $LaAlO_3$ coating. J Alloy Compd 766:546–555

35. Zheng H, Chen X, Yang Y, Li L, Li G, Guo Z, Feng C (2017) Self-assembled $LiNi_{1/3}Co_{1/3}Mn_{1/3}O_2$ nanosheet cathode with high electrochemical performance. ACS Appl Mater Interfaces 9:39560–39568

36. Li Z, Cao S, Wu C, Li H, Chen J, Guo W, Chang B, Shen Y, Bai Y, Wang X (2022) A facile and high-effective oxygen defect engineering for improving electrochemical performance of lithium-rich manganese-based cathode materials. J Power Sources 536:231456

37. Chen GR, An J, Meng YM, Yuan CZ, Matthews B, Dou F, Shi LY, Zhou Y, Song PG, Wu G, Zhang DS (2019) Cation and anion Co-doping synergy to improve structural stability of Li- and Mn-rich layered cathode materials for lithium-ion batteries. Nano Energy 57:157–165

38. Zhao LN, Chen GR, Weng YH, Yan TT, Shi LY, An ZX, Zhang DS (2020) Precise Al_2O_3 Coating on $LiNi_{0.5}Co_{0.2}Mn_{0.3}O_2$ by atomic layer deposition restrains the shuttle effect of transition metals in Li-ion capacitors. Chem Eng J 401:126138